Korean J. Chem. Eng., 37(4), 577-582 (2020)
DOI: 10.1007/s11814-020-0476-7

pISSN: 0256-1115
eISSN: 1975-7220

RAPID COMMUNICATION

Experimental investigation of charge transfer coefficient and exchange current density in standard fuel cell model for polymer electrolyte membrane fuel cells

Hyungwook Lee‡, Changhee Han‡, and Taehyun Park†

School of Mechanical Engineering, Soongsil University, 369 Sangdo-ro, Dongjak-gu, Seoul 06978, Korea
(*Received 10 September 2019 • accepted 29 December 2019*)

Abstract−Two representative parameters, exchange current density (j_0) and charge transfer coefficient (α), in a standard fuel cell model of polymer electrolyte membrane fuel cells (PEMFCs) were experimentally investigated. The polarization characteristics and the corresponding electrochemical impedance spectra of the normal PEMFCs were measured and Tafel curves were calculated from them, where j_0 and α were finally calculated. As a result, the calculated j_0 was 0.11-0.70 A/cm^2, while the α was 0.056-0.023, depending on the operating temperature. Here, the j_0 is extremely overestimated while α is underestimated as compared with those in literature. Although the reason for such difference is not clear, it is expected that it could affect the predicted performance by the model significantly if the fuel cell performance is improved highly in the future so the activation overvoltage corresponding to identical current is lowered.

Keywords: Polymer Electrolyte Membrane Fuel Cell, Charge Transfer Coefficient, Exchange Current Density, Fuel Cell Model, Electrochemical Impedance Spectroscopy

INTRODUCTION

Polymer electrolyte membrane fuel cells (PEMFCs) have been highlighted as a promising future power source due to their high energy/power density, high energy conversion efficiency, excellent scalability, and cleanliness [1-3]. The technological level of the PEMFCs recently reached commercialization level, and several applications such as portable power sources, fuel cell electric vehicles, and PEMFC-based power plant already have been released in the market [1,4-7]. Along with this development, many researchers have developed a simulation model for this PEMFC to understand the deep electrochemical science inside the fuel cells [1,8-14]. Here, most of the fuel cell simulation models in literature have been based on the 1-dimensional standard fuel cell model, which can be represented as the following Eq. (1):

$$V = E^0 - \eta_{act} - \eta_{ohmic} - \eta_{conc} \tag{1}$$

where V, E^0, η_{act}, η_{ohmic}, and η_{conc} represent the voltage, standard potential of the fuel cell without current, activation overvoltage, ohmic overvoltage, and concentration overvoltage, respectively. The activation, ohmic, and concentration overvoltage could be calculated from the following Eqs. (2), (3), and (4).

$$j + j_{leak} = j_0 \left\{ \exp\left(\frac{\alpha z F \eta_{act}}{RT}\right) - \exp\left(\frac{-(1-\alpha) z F \eta_{act}}{RT}\right) \right\} \tag{2}$$

$$\eta_{ohmic} = (ASR) j \tag{3}$$

$$\eta_{conc} = c \ln\left(\frac{j_L}{j_L - (j + j_{leak})}\right) \tag{4}$$

Here, j, j_{leak}, j_0, α, z, F, R, T, (ASR), c, and j_L indicate current density, leakage current density, exchange current density, charge transfer coefficient, number of electrons transferred in the reaction, Faraday constant, ideal gas constant, temperature at which the reaction occurs, area-specific resistance, empirical constant of the mass transport, and limiting current density, respectively. Eq. (2), i.e. the Butler-Volmer equation, assumes that there is little concentration gradient of reactants and byproducts at each electrode. This model is considered as the simplest way to describe the electrochemical behavior and, finally, the corresponding performance of the fuel cells. However, the problem comes with two parameters: α and j_0. It is because other parameters except α and j_0 can be measured and/or fixed, while those two should be assumed or referred from other fuel cell experiment of different testing conditions. The c and j_L should also be predicted empirically, but they are different from α and j_0 in that c and j_L cannot be standardized because they depend more significantly on the experimental conditions such as the flow rate, humidity, flooding, and so forth [15]. The α is explained elsewhere [16]: It is a measure of the symmetry of the energy barrier in free energy curves of reaction, and high α means fast reaction kinetics. Meanwhile, the current density means at which the forward and backward exchange current densities are at equilibrium [13]. It indicates that all such parameters are related to the electrochemical reaction kinetics and also significant to describe the fuel cell performance precisely. However, most of the research including this standard fuel cell model supposes α and j_0 as some specific values based on other researches [11,14,17].

Even the most frequently used values of α and j_0 in the standard fuel cell model are 0.3 (anode)/0.5 (cathode) and 0.1 (anode)/10^{-4} (cathode) A/cm^2, respectively. Unfortunately, to our knowledge, it could not be highly accurate because they are based on a half-cell test with the well-defined flat and fine interface between electrode and electrolyte [17]. This condition is highly different from the real

†To whom correspondence should be addressed.
E-mail: taehyunpark@ssu.ac.kr
‡These authors contributed equally to this work.

operating conditions of fuel cells.

This study hence reports the variation of α and j_0 in terms of fuel cell operating conditions, and monitors them precisely under the variation of operating temperature and the loading of Pt. Because the previous reports discussing this stand fuel cell model describe the electrochemical interface as simply "flat" structure. However, the theoretical electrochemistry and so-called "3-D structured Pt/C based catalyst layer" of the fuel cell are different from each other [18]. Therefore, this study employs the representative catalyst structure of PEMFC by fabricating the catalytic layer through Pt/C-based ink spray, which is a progressive structure of flat electrode/electrolyte interface in normal electrochemistry so as to maximize the reactive sites and obtain maximal performance from the constrained volume and weight of catalyst layer in PEMFCs. Here, this study especially controls two control parameters: operating temperature and the loading of Pt. Those are diversified and the resulting electrochemical behaviors are investigated by measuring polarization curves and corresponding electrochemical impedance spectra (EIS). Tafel curves are finally calculated and α and j_0 are finally extracted from the Tafel plots.

EXPERIMENTAL

Membrane-electrode assemblies (MEAs) were fabricated throughout this study as follows: Nafion® 212 membrane (Dupont Inc., USA) was used for all tests. It was mounted on a hot vacuum plate (CNL Inc., Republic of Korea) to deposit catalyst layer on both sides of the membrane. The temperature of the hot vacuum plate was maintained at 80 °C. The catalyst ink was prepared as follows: Pt/C (40 wt% Pt, Johnson Matthey Inc., UK), Nafion® ionomer solution (5 wt%, Sigma Aldrich Inc., USA), and isopropyl alcohol (IPA, Daejung Chemicals and Metals Co., Republic of Korea) were mixed and sonicated at room temperature for 5 min. The weight ratio of Pt and Nafion was 1 : 1.27. This ink was sprayed onto Nafion®-mounted hot vacuum plate. The reactive area was 2.24× 2.24 cm^2 (Total area of 5 cm^2). By varying the amount of ink, the MEAs of four different Pt loading (0.12, 0.24, 0.36, and 0.48 mg/cm^2) were prepared. The MEA was sandwiched by two gas-diffusion layers (GDLs, 39BC, Sigracet Inc., Germany) with micro-porous layers. It was then assembled in a PEMFC unit cell with two polytetrafluoroethylene-coated cloth gaskets. The depth, rib width, and channel width were all 1 mm.

The electrochemical performance of the PEMFC with the as-fabricated MEA was measured as follows: Fully humidified hydrogen and oxygen were supplied to the anode and cathode of the fuel cell, respectively. The volumetric flow rates of hydrogen and oxygen were 150 and 600 cm^3/min, respectively. Before testing, the fuel cell was activated by measuring the current-voltage repeatedly, and the final current-voltage (I-V) curve where the repeatedly measured I-V curve converged was selected. The I-V curve was measured by starting from the open-circuit voltage (OCV) and the current was swept by 0.1 A/s. After measuring the polarization characteristics, the corresponding EIS was investigated using an electrochemical workstation (ZIVE SP2, WonA Tech Co., Republic of Korea). The sinusoidal voltage input at OCV and 0.80 V with the amplitude of 0.03 V was applied to the fuel cell and the corresponding current response was monitored. The results were all visualized on Nyquist plot. Total four MEAs with the Pt loading of 0.12, 0.24, 0.36, and 0.48 mg/cm^2 were tested and each MEA was tested at 50 and 80 °C. As a result, total eight I-V curves and corresponding total sixteen EIS were obtained throughout the experiment.

The α and j_0 were calculated as follows: the I-V curve was first calibrated by subtracting the leakage current, and the ohmic resistance was caculated from the Nyquist plot (The left intersect of the half circle with Z_{Re}-axis). The ohmic-free I-V curve was then calculated by summing the ohmic overvoltage on both sides of Eq. (1). Subsequently, it was converted to Tafel plot (converting horizontal axis to ln(j) instead of j in I-V curve) and the slope and the intersect with ln(j) axis were calculated by using Matlab R2018b software. From the calculated values, the α and j_0 were finally extracted from the slope and the intersect, respectively, using the Tafel equation converted from Eq. (2).

RESULTS AND DISCUSSION

The EIS of the as-prepared PEMFCs is indicated in Fig. 1. Theoretically, the EIS of the fuel cell can be expressed as two interfacial double layers (Anode and cathode) and one ohmic resistance which is induced mainly by the ionic conductivity of an electrolyte membrane. According to an equivalent circuit model in electrochemistry, the double layer can be presented as a parallel connection of constant phase element (CPE) and charge transfer resistance (R_{ct}), which is indicated as insets of Fig. 1. However, the anodic charge transfer behavior could be ignored in normal hydrogen-supplied fuel cell due to the extremely fast kinetics of hydrogen oxidation reaction at the anode than that of oxygen reduction reaction at the cathode (Note the representive exchange current densities in anode and cathode of standard PEMFC are 0.1 and 10^{-4} A/cm^2 as mentioned in the introduction). It becomes more clear as considering Tafel equation derived from Eq. (2), which is represented as follows:

$$\eta_{act} = \frac{RT}{\alpha zF}\{\ln(j) - \ln(j_0)\} \quad (5)$$

According to Eq. (5), small exchange current density at the cathode would bear large activation overvoltage and such overvoltage dominates the total activation overvoltage. Therefore, the anodic interfacial double layer could be ignored and only one cathodic double layer is indicated in the insets of Fig. 1.

The variation of the charge transfer resistance with the change of temperature and Pt loading is also well-matched theoretically. Here, the operating temperatures were set to 50 and 80 °C because the standard PEMFCs present highest performance at about 80 °C and it is maintained at about 50 °C (not stack operation but in the case of unit cell operation) if operated without external temperature controlling system by the heat generation itself. A clear decrease of the charge transfer resistance with increasing operating temperature (50 °C *vs.* 80 °C) is observable in Fig. 1(a) and (b), and although not clearly visualized, the charge transfer resistance in Fig. 1(c) and (d) also decreases with the increasing operating temperature. It means that the reaction kinetics inside the anode and cathode became faster as the operating temperature increased. It coincides

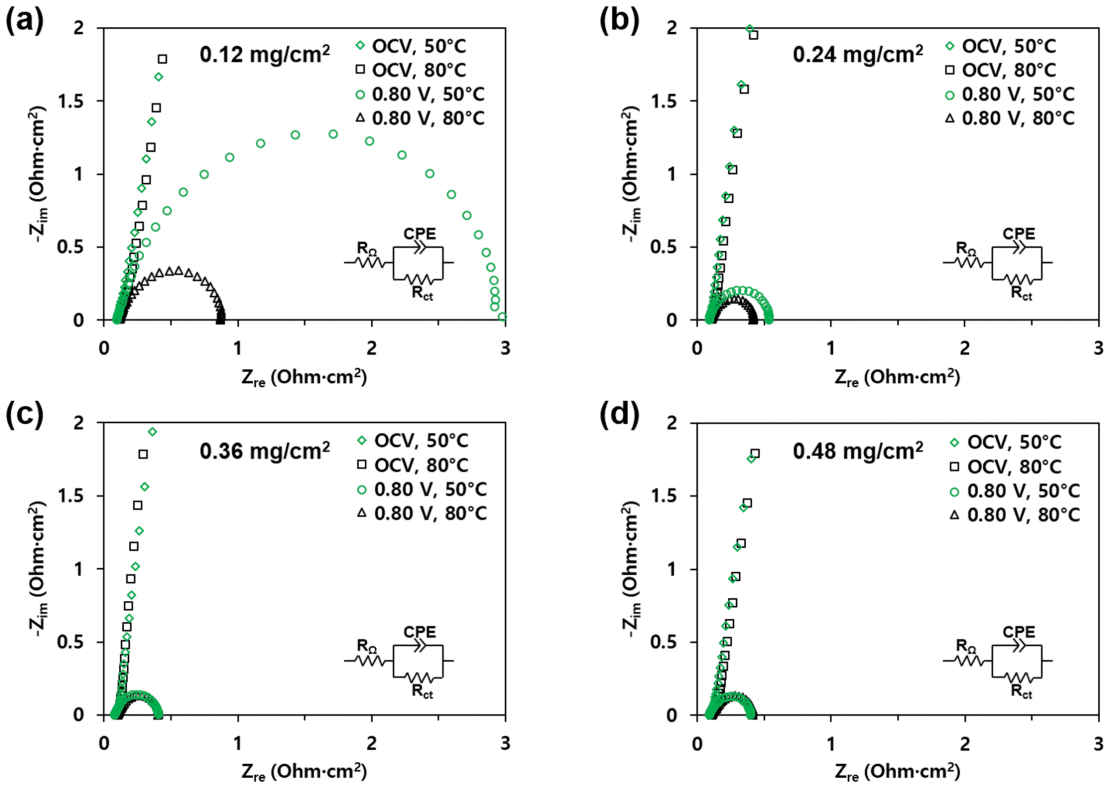

Fig. 1. EIS of the PEMFCs operating at 50 and 80 °C with the Pt loading of (a) 0.12, (b) 0.24, (c) 0.36, and (d) 0.48 mg/cm². All the spectra were measured at OCV and 0.80 V *vs.* RHE.

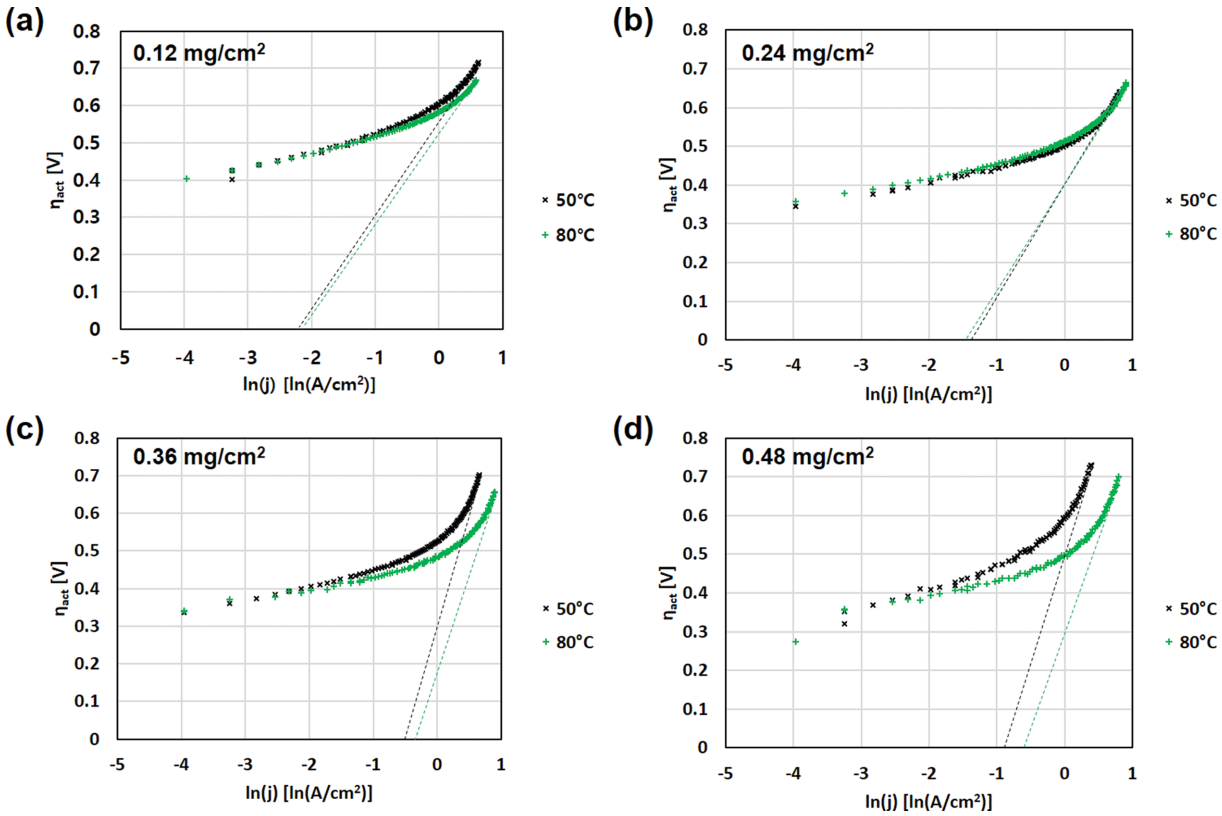

Fig. 2. Tafel plots of the PEMFCs operating at 50 and 80 °C with the Pt loading of (a) 0.12, (b) 0.24, (c) 0.36, and (d) 0.48 mg/cm². The dashed lines are the asymptotes of the curves at high activation overvoltages (>0.6 V).

with the characteristics derived from Eqs. (2) and (5) that the increase of the temperature reduces the activation overvoltage, which is also visualized in Fig. 2 and discussed later. When it comes to the loading of Pt, it is expected the high loading of Pt would reduce the charge transfer resistance. In real, it is clearly visualized in Fig. 1 that the diameter of the half circles decreases from the case in Fig. 1(a) to (d). Importantly, the ohmic resistances at all cases were calculated in order to convert all the I-V characteristics to Tafel plots. The ohmic resistances including the external wiring resistances are 0.110 and 0.092 Ω·cm^2 at 50 and 80 °C, respectively. The reason why the wiring resistance was not compensated is to secure the reliability of Tafel curves. Only the activation overvoltage should be represented in Tafel plot and such includes the deletion of wiring resistance.

By obtaining the ohmic resistances, the I-V characteristics were processed to obtain the α and j_0 as shown in Fig. 2. Although not shown, it was confirmed before converting to Tafel plots that there was no significant problem of sealing by monitoring the variations of OCVs, which were all stable at the range from 0.91 to 0.97 V. The OCV shows relatively high values (0.97 V) in the PEMFC with high Pt loading (0.48 mg/cm^2), which is believed to be the difference of strong polarization at anode and cathode by the high amount of Pt (Note high Pt with large surface area would bear a clear polarization in all electrochemical cells. Recall Nernst equation representing the OCV of any fuel cells) [13,16]. As mentioned, the activation overvoltage will be decreased if the operating temperature or the loading of Pt is increased, according to Eq. (5). In reality, all the curves measured at 80 °C are positioned beneath the curves at 50 °C in Fig. 2. Although the Tafel curves in Fig. 2(b) were not separated clearly, it seems to be an measurement error and does not lie out of the tendency, which will be discussed later. The j_0 could be obtained from the intersect of the asymptote extrapolated from the Tafel curve at high current density with ln(j)-axis, which is shown as dashed line in Fig. 2. In addition, the α can be obtained from the slopes of asymptotes by using Eq. (5), as indicated in Table 1.

The variation of α and j_0 with respect to operating temperature and the loading of Pt are re-plotted in Fig. 3. It was first expected that the exchange current density would increase with increasing the loading of Pt because the addition of Pt could expand the electrochemically reactive area. However, Fig. 3(a) shows that it increases with increasing Pt upto 0.36 mg/cm^2 and then slightly decreases at all operating temperatures. It is speculated that such phenomenon actually means the "effectiveness" of the addition of Pt. The effectiveness of the Pt is maximized with the Pt loading of 0.36 mg/cm^2, which is then decreased by the disturbance of the reactants diffusion by the increased thickness of diffusion medium [19-21]. Especially, Marr et al. reported that fuel cell reactions occur in a thin catalytic layer a few micrometers thick, suggesting the efficacy of the Pt catalyst, which corresponds well with the results of this study [22]. In addition, according to the dependence of the exchange current density on temperature suggested by Parthasarathy et al., the difference ratio between j_0 at 50 and 80 °C should be constant [23]. It is also believed that such inconsistency represents the effectiveness of Pt as described above.

Here, it is noticeable that the absolute values of j_0 (0.11-0.70 A/cm^2 in Fig. 3(a)) are quite higher from others in literature, especially considering that the cathodic reaction inside the PEMFC dominates the activation overvoltage [22-26]. It is also distinguished from the value of j_0 suggested elsewhere [13]. However, there is no doubt that the standard fuel cell model with the j_0 and α, would be fitted well with the I-V curve because they are all mathematically extracted from the I-V curve itself, meaning calculating the standard fuel cell model with them is same as retrieving to the original form. Then how could the overestimated j_0 be compensated to shoot the original data? It is by the charge transfer coefficient in Fig. 3(b). Both j_0 and α indicate the electrochemical kinetics inside a fuel cell and high values mean fast kinetics. Then the charge transfer coefficient, α, should be underestimated to compensate the difference with the conventional values. In reality, α ranges from

Table 1. Slopes of asymptotes in Fig. 2

Slopes of asymptotes in Tafel plot		Loading of Pt (mg/cm^2)			
		0.12	0.24	0.36	0.48
Operating temperature	50 °C	0.055691	0.048009	0.024005	0.025314
	80 °C	0.056827	0.050628	0.027845	0.029623

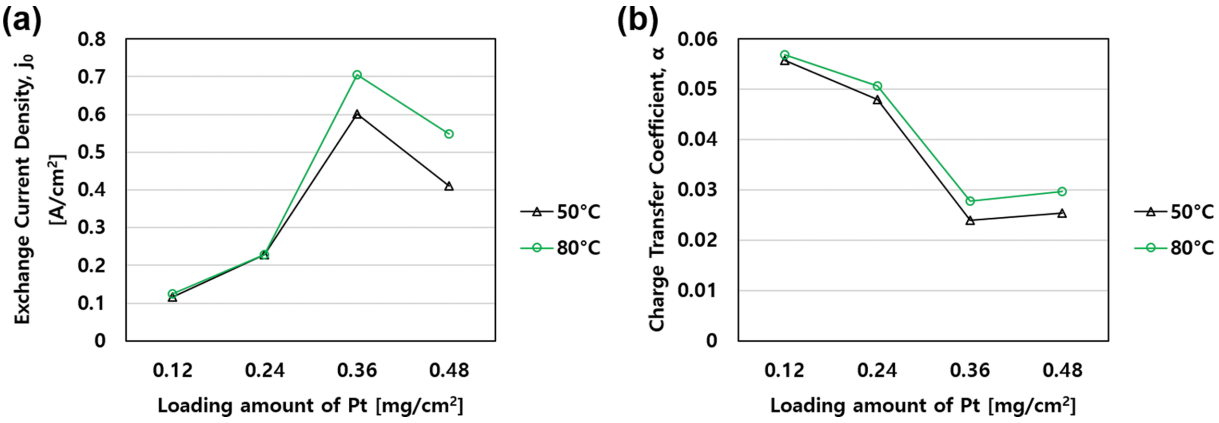

Fig. 3. Variations of (a) exchange current density and (b) charge transfer coefficient of the PEMFCs with Pt loadings of 0.12, 0.24, 0.36, and 0.48 mg/cm^2.

0.056 to 0.023 in Fig. 3(b), and it is an order of the magnitude lower than the values used to model normal PEMFCs [22-26]. There is no doubt that ignoring the backward reaction term in Eq. (2), i.e., ignoring the second exponential term, does not affect the result here. It is because the exponentials inside the first and second exponential terms are 9.777×10^{9} and 1.023×10^{-10}, respectively, if α, z, F, η_{act}, R, and T are set to 2, 96485 C/mol, 0.5, 0.7 V, 8.314 J/mol·K, and 353.15 K, respectively. The forward term is more than 10^{20} times than the backward term, meaning that ignoring the backward term is highly reasonable. Even the commonly known α (0.3-0.5) was first reported by controlling the microscale interface between Pt and Nafion® which is precisely controlled experimentally [23]. The electrochemically reactive site in normal PEMFCs is composed of carbon-supported nanoscale platinum, while the experiment in [23] is dense 100-μm-thick platinum electrode on Nafion® membrane. Even the experiments for estimating j_0 and α were conducted with pure oxygen at relatively high pressure, which is believed that the experimental conditions are totally different from the real PEMFC. Another reason for such mismatch could be the ignorance of the concentration loss, η_{conc}, in Eq. (1) since this loss is also derived partially from the concentration terms of the detailed form of Butler-Volmer equation (Concentrations not shown in Eq. (2)). However, to our knowledge, no report has elaborated upon the physics and meanings of the charge transfer coefficient describing fuel cells. Only few reports can be found showing the disjunction between the experimental and theoretical parameters [27].

Nevertheless, it is obvious throughout this research that the j_0 and α calculated from the ohmic-free I-V curve of the PEMFC are not well matched to conventional values in literature. The conventional values could be used for the parameters in standard fuel cell model for PEMFC. But it is speculated that using them would bear a big error at high current density region due to the characteristics of the exponential relation. It means that the standard fuel cell model will not be used for high-performance PEMFC in the future because the conventional α and j_0 might induce exaggerated Butler-Volmer behavior. Thus, such difference could be lowered if high activation overvoltage is measured. Unfortunately, PEMFCs operate under a voltage of <1.2 V, meaning that is impossible. Additional experiments should be designed and conducted to further investigate the exact relation between Butler-Volmer behavior and the charge transfer resistance.

CONCLUSION

The charge transfer resistance, j_0, and charge transfer resistance, α, were investigated in order to describe the electrochemical polarization behavior of the PEMFC based on the standard fuel cell model. The I-V characteristics and corresponding EIS were investigated and Tafel curves were calculated based on the experimental results. As a result, the j_0 was calculated to be 0.11-0.70 A/cm^2, while the α was 0.056-0.023, varying based on the operating temperature. The j_0 is very higher but α very lower than the values in literature. Although the difference between the conventional values and the measured values in this study would not bear the big error between the data predicted by standard fuel cell model and the experimental data, it is thought that such conventional data would have some problems if the performance of current PEMFC was highly improved and induced a big difference between activation overvoltage and current density in Butler-Volmer behavior. Although not clearly explained where such disjunction comes from, additional investigation seems required to further understand the deep science inside the electrochemistry of the PEMFCs.

ACKNOWLEDGEMENT

This work was supported by the Soongsil University Research Fund of 2018.

NOMENCLATURE

V	: voltage
E^0	: standard potential of the fuel cell at zero current
η_{act}	: activation overvoltage
η_{ohmic}	: ohmic overvoltage
η_{conc}	: concentration overvoltage
j	: current density
j_{leak}	: leakage current density
j_0	: exchange current density
α	: charge transfer coefficient
z	: number of electron transferred
F	: faraday constant
R	: ideal gas constant
T	: temperature at which the reaction occurs
(ASR)	: area-specific resistance
c	: empirical constant of the mass transport
j_L	: leakage current density
CPE	: constant phase element
R_{ct}	: charge transfer resistance

REFERENCES

1. A. Dicks and D. Rand, *Fuel cell systems explained*, Wiley, New York (2018).
2. M. Winter and R. J. Brodd, *Chem. Rev.*, **104**(10), 4245 (2004).
3. C. K. Dyer, *J. Power Sources*, **106**(1-2), 31 (2002).
4. J. H. Wee, *Renew. Sustain. Energy Rev.*, **11**(8), 1720 (2007).
5.. Y. Wang, K. S. Chen, J. Mishler, S. C. Cho and X. C. Adroher, *Appl. Energy*, **88**(4), 981 (2011).
6. L. van Biert, M. Godjevac, K. Visser and P. V. Aravind, *J. Power Sources*, **327**, 345 (2016).
7. G. Hoogers, *Fuel cell technology handbook*, CRC Press, Florida (2003).
8. S. Yazar, E. Kurtulbas, S. Ortaboy, G. Atun and S. Sahin, *Korean J. Chem. Eng.*, **36**(7), 1184 (2019).
9. I.-S. Han, S.-K. Park and C.-B. Chung, *Korean J. Chem. Eng.*, **33**(11), 3121 (2016).
10. C. S. Lee and S. C. Yi, *Korean J. Chem. Eng.*, **21**(6), 1153 (2004).
11. D. M. Bernardi and M. W. Verbrugge, *J. Electrochem. Soc.*, **139**(9), 2477 (1992).
12. T. E. Springer, T. A. Zawodzinski and S. Gottesfeld, *J. Electrochem. Soc.*, **138**(8), 2334 (1991).
13. R. O'Hayre, S.-W. Cha, W. Colella and F. B. Prinz, *Fuel cell fundamentals*, Wiley, New York (2009).

14. P. T. Nguyen, T. Berning and N. Djilali, *J. Power Sources*, **130**(1-2), 149 (2004).
15. T. E. Springer, *J. Electrochem. Soc.*, **138**(8), 2334 (1991).
16. A. J. Bard and L. R. Faulkner, *Electrochemical methods: fundamentals and applications*, Wiley, New York (2001).
17. A. Parthasarathy, S. Srinivasan, A. J. Appleby and C. R. Martin, *J. Electroanal. Chem.*, **339**(1-2), 101 (1992).
18. S. Litster and G. McLean, *J. Power Sources*, **130**(1-2), 61 (2004).
19. V. A. Paganin, E. A. Ticianelli and E. R. Gonzalez, *J. Appl. Electrochem.*, **26**(3), 297 (1996).
20. Y. Qi, B. Huang and K. T. Chuang, *J. Power Sources*, **150**, 32 (2005).
21. L. R. Jordan, A. K. Shukla, T. Behrsing, N. R. Avery, B. C. Muddle and M. Forsyth, *J. Power Sources*, **86**(1-2), 250 (2000).
22. C. Marr and X. Li, *J. Power Sources*, **77**(1), 17 (1999).
23. A. Parthasarathy, S. Srinivasan, A. J. Appleby and C. R. Martin, *J. Electrochem. Soc.*, **139**(9), 2530 (1992).
24. K. Broka and P. Ekdunge, *J. Appl. Electrochem.*, **27**(3), 281 (1997).
25. T. E. Springer, T. A. Zowodzinski and S. Gottesfeld, *J. Electrochem. Soc.*, **138**(8), 2334 (1991).
26. S. Um, C. Y. Wang and K. S. Chen, *J. Electrochem. Soc.*, **147**(12), 4485 (2000).
27. T. Park, I. Chang, J. H. Jung, H. B. Lee, S. H. Ko, R. O'Hayre, S. J. Yoo and S. W. Cha, *Energy*, **134**, 412 (2017).